A Tetrazolyl-Substituted Subtype-Selective AMPA Receptor Agonist[⊥]

Stine B. Vogensen,[†] Karla Frydenvang,[†] Jeremy R. Greenwood,[†] Giovanna Postorino,[†] Birgitte Nielsen,[†] Darryl S. Pickering,[‡] Bjarke Ebert,[§] Ulrik Bølcho,[⊗] Jan Egebjerg,[§] Michael Gajhede,[†] Jette S. Kastrup,[†] Tommy N. Johansen,[†] Rasmus P. Clausen,[†] and Povl Krogsgaard-Larsen*[,†]

Department of Medicinal Chemistry and Department of Pharmacology and Pharmacotherapy, The Faculty of Pharmaceutical Sciences, University of Copenhagen, 2 Universitetsparken, DK-2100 Copenhagen, Denmark, Department of Molecular and Structural Biology, University of Aarhus, Denmark, and Department of Electrophysiology, H. Lundbeck A/S, 9 Ottiliavej, DK-2500 Valby, Denmark

Received December 17, 2006

Replacement of the methyl group of the AMPA receptor agonist 2-amino-3-[3-hydroxy-5-(2-methyl-2*H*-5-tetrazolyl)-4-isoxazolyl]propionic acid (2-Me-Tet-AMPA) with a benzyl group provided the first AMPA receptor agonist, compound **7**, capable of discriminating GluR2−4 from GluR1 by its more than 10-fold preference for the former receptor subtypes. An X-ray crystallographic analysis of this new analogue in complex with the GluR2-S1S2J construct shows that accommodation of the benzyl group creates a previously unobserved pocket in the receptor, which may explain the remarkable pharmacological profile of compound **7**.

Introduction

(*S*)-Glutamic acid (Glu) is the main excitatory neurotransmitter in the mammalian central nervous system (CNS).[1,2] Glu exerts its effects through two types of receptors: ligand-gated ionotropic receptors (iGluRs) and G-protein-coupled metabotropic receptors (mGluRs). The iGluRs are central players in rapid neural signaling and are important in many CNS functions, including learning and memory.[3] Thus, iGluRs are considered potential therapeutic targets in a number of neurological and psychiatric disorders.[4] The iGluRs are classified based on their selective recognition of the three agonists *N*-methyl-D-aspartic acid (NMDA), (*S*)-2-amino-3-(3-hydroxy-5-methyl-4-isoxazolyl)-propionic acid [(*S*)-AMPA, **1**] (Figure 1), and kainic acid (KA). Functional iGluRs assemble as homo- or heteromeric tetramers of iGluR subunits. Seven NMDA subunits (NR1, NR2A-D, NR3A,B), four AMPA subunits (GluR1−4), and five KA subunits (GluR5−7, KA1,2) have been cloned and characterized. Structural insights to the activation of iGluRs have been obtained from X-ray crystallographic analyses of various agonists and antagonists bound to soluble constructs of the S1S2 ligand-binding domain (LBD) from several of the iGluR subunits, notably of GluR2.[5] These structures show that the LBD is like a clamshell that closes around agonists, presumably leading to opening of the receptor ion-channel. Furthermore, a correlation has been found between the agonist efficacy and the degree of LBD closure induced by the agonists, whereas antagonists seem to stabilize the unbound open LBD structure.

The development of subtype selective AMPA receptor ligands is of high relevance to CNS diseases. As an example, variants of the GRIA1 gene, which codes for the GluR1 AMPA receptor subunit, have been reported to be associated with certain forms of schizophrenia.[6] In the search for such ligands for studies of the physiological role and pharmacological characteristics of the AMPA receptors, much research has been focused on the development of potent and selective agonists. One of the most potent AMPA agonists is (*S*)-2-amino-3-[3-hydroxy-5-(2-methyl-2*H*-5-tetrazolyl)-4-isoxazolyl]propionic acid [(*S*)-2-Me-Tet-AMPA, **2**].[7,8] However, compound **2** shows little selectivity among GluR1−4 based on receptor affinity studies using cloned homomeric AMPA receptors expressed in Sf9 insect cells.[9] Replacements of the methyl group of 2-Me-Tet-AMPA with larger groups such as 2-ethyl (**3**), 2-propyl (**4**), and 2-isopropyl (**5**) (Figure 1) do not result in any significant increase in selectivity.[9]

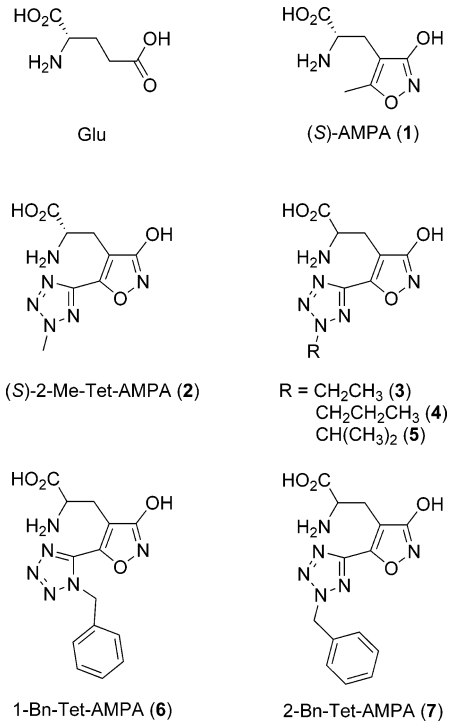

Figure 1. Chemical structures of (*S*)-glutamic acid (Glu), (*S*)-AMPA (**1**), the AMPA agonist (*S*)-2-Me-Tet-AMPA (**2**), 2-Et-Tet-AMPA (**3**), 2-Pr-Tet-AMPA (**4**), 2-Pr^i-Tet-AMPA (**5**), and the new 1-Bn-Tet-AMPA (**6**) and 2-Bn-Tet-AMPA (**7**).

Unlike the preceding results for AMPA analogues, high selectivity in the functional activation of and affinity for GluR1/2

[⊥] PDB ID: 2P2A.

* Author to whom correspondence should be addressed. Phone: +45 35306511; Fax: +45 35306040; E-mail: pkl@carlsbergfondet.dk.

[†] Department of Medicinal Chemistry, University of Copenhagen.

[‡] Department of Pharmacology and Pharmacotherapy, University of Copenhagen.

[⊗] University of Aarhus.

[§] H. Lundbeck A/S.

10.1021/jm061439q CCC: $37.00
Published on Web 04/25/2007

Scheme 1[a]

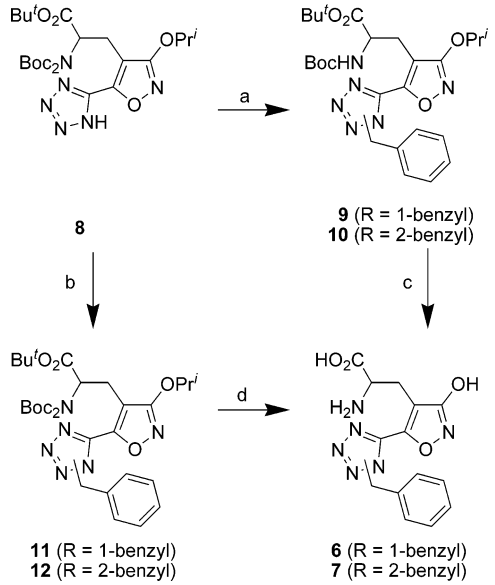

[a] Reagents and conditions. (a) *O*-benzyl *S*-propargyl xanthate,[12] toluene, reflux; (b) benzyl alcohol, triphenylphosphine, DIAD; (c) 48% aq HBr, reflux (only compound **7** isolated); (d) BBr_3, −78 °C.

GluR3/4 has previously been demonstrated for (*RS*)-2-amino-3-(4-chloro-3-hydroxy-5-isoxazolyl)propionic acid (Cl-HIBO).[10] It was suggested that tyrosine 702 in GluR2 (Y716 in GluR1) is the most likely structural determinant explaining the observed selectivity.[10,11] GluR3 and -4 contain a phenylalanine residue in equivalent positions. Apart from this sequence difference, the ligand-binding pocket is highly conserved, and previous X-ray crystallographic analyses have given little insight into how nonconserved residues outside the binding pocket might be reached by AMPA receptor agonists and exploited for selectivity.

Here, we report the synthesis and pharmacological characterization of a new selective AMPA receptor agonist (*RS*)-2-amino-3-[3-hydroxy-5-(2-benzyl-2*H*-5-tetrazolyl)-4-isoxazolyl]-propionic acid (2-Bn-Tet-AMPA, **7**) (Figure 1). Furthermore, we report the X-ray structure of this analogue in complex with the GluR2-S1S2J construct.

Results

Chemistry. Benzylation of the previously reported tetrazole[9] **8** with *O*-benzyl *S*-propargyl xanthate[12] gave a 1:2 mixture of the N-benzylated 1- and 2-regioisomers (**9** and **10**) with concomitant loss of one Boc protecting group (Scheme 1). The same ratio of regioisomers (**11** and **12**) was observed when benzylation was performed using Mitsunobu conditions with benzyl alcohol, but under these reaction conditions at ambient temperature, both of the thermolabile Boc protecting groups persisted. Contrary to the previously reported series of 1- and 2-alkyltetrazolyl-AMPA analogues,[9] the benzyl regioisomers **9** and **10** or **11** and **12** could not be separated at this stage. Initially, we used previous deprotection conditions involving hydrogen bromide on the mixture of regioisomers, which afforded a single regioisomer, albeit in low yield. The X-ray crystallographic analysis of the isolated regioisomer cocrystallized with the soluble construct of the LBD of GluR2 enabled an unambiguous regioisomeric structure determination of 2-Bn-Tet-AMPA (**7**). The 1-regioisomer (1-Bn-Tet-AMPA, **6**) had undergone complete debenzylation to give the free tetrazole. However, we found that deprotection with boron tribromide rather than hydrogen bromide enabled the selective removal of all protecting groups, including the *O*-isopropyl group, while maintaining the *N*-benzyl groups of both regioisomers, which were separated using HPLC.

Table 1. Receptor Binding Affinities and Electrophysiological Data at Native iGluRs[a]

	receptor binding			electrophysiology
compd	[^{3}H]AMPA, IC_{50} (μM)	[^{3}H]KA, IC_{50} (μM)	[^{3}H]CGP 39653, K_i (μM)	cortical wedge, EC_{50} (μM)
(*RS*)-**1**	0.039[b]	>100[b]	>100	3.5[b]
2[b]	0.009	11	>100[c]	0.11
3[d]	0.13	> 100	>100	3.5
4[d]	2.5	> 100	>100	32
5[d]	6.2	> 100	>100	71
6	>100	> 100	>100	nd
7	2.7 [2.5; 2.9]	>100	87 [79; 96]	32 [31; 33]

[a] Values are expressed as the antilog to the logarithmic mean of at least three individual experiments. The numbers in brackets [min; max] indicate ± SEM according to a logarithmic distribution. nd, not determined. [b] Reference 8. [c] The radioligand used was ^{3}[H]CPP. [d] Reference 9.

In Vitro Pharmacology. Initially, the binding affinities of **6** and **7** for the three classes of native iGluRs were determined using the radioligands [^{3}H]AMPA,[13] [^{3}H]KA,[14] and [^{3}H]CGP 39653[15] (NMDA receptors) in binding assays using a rat brain synaptosomal preparation[16] (Table 1). Like the AMPA 5-(2-alkyltetrazolyl) analogues,[9] compound **7** showed an affinity for [^{3}H]AMPA binding sites similar to that of **4**. Unlike members of the alkyl series, **7** showed weak affinity for NMDA receptor sites. The 1-isomer, compound **6**, showed no measurable affinity at native iGluRs (Table 1) in accordance with previous results on 1-alkyltetrazolyl AMPA analogues.[7−9] The binding affinity profile of **7** for a range of AMPA and KA iGluR subtypes (GluR1−GluR6) was investigated by homomeric expression of these receptor subtypes in *Sf9* insect cells[10] (Table 2). In this series of experiments, compound **7** showed more than 10-fold selectivity toward GluR2−4 compared to GluR1.

A modified version[17] of the previously described rat cortical wedge preparation[18] was used as an in vitro electrophysiological model in which **7** displayed agonist activity (Table 1). When comparing with compounds **2**−**5**, the potency and affinity of **7** and **4** are of similar magnitude (Table 1).

These results, combined with the high degree of domain closure in the X-ray crystal structure of **7** in GluR2 described below, prompted a further functional characterization to determine the agonist efficacy of **7** at GluR2. This was done using two electrode voltage clamp measurements on *Xenopus laevis* oocytes expressing the non-desensitizing homomeric GluR2 (L483Y) mutant (Figure 2). In this assay, application of saturating concentration of **7** was able to induce a maximal current of 84% relative to the maximal Glu-induced current and exhibited an EC_{50} value of 95 μM [87; 103].

X-ray Crystallographic Analysis. The GluR2 LBD (GluR2-S1S2J) was crystallized as a dimer containing Glu in molA and (*S*)-**7** in molB. This heterodimeric structure was refined to 2.26 Å resolution (Figure 3). The size of the dimer interface is ca. 950 Å^2 (molA 952 Å^2 and molB 953 Å^2) of buried solvent accessible surface (see Supporting Information for further details regarding the interface). Ligand-binding data showed that the GluR2-S1S2J protein reproduced the binding characteristics of **7** at the membrane-bound receptors. The α-carboxylate and the α-ammonium group of (*S*)-**7** in GluR2-S1S2J are positioned in the same consistent manner as previously described for similar amino acid ligands.[11,19] Unlike the conserved binding pattern for the amino acid moiety, variable orientations have been reported for the isoxazole rings of the substituted AMPA analogues.[11,20] In the present structure, both heterocyclic rings are situated in the same position as previously observed in a

Table 2. Receptor Binding Affinity at Cloned Subtypes Expressed in *Sf9* Cells[a]

	receptor affinity (K_i in μM)					
compd	GluR1	GluR2	GluR3	GluR4	GluR5	GluR6
(*RS*)-**1**[b]	0.022 ± 0.004	0.017 ± 0.003	0.021 ± 0.003	0.040 ± 0.020	1.2 ± 0.1	>1000
2[b]	0.0052 ± 0.0004	0.0039 ± 0.0009	0.0022 ± 0.0001	0.0027 ± 0.0003	0.081 ± 0.003	19 ± 4
3[b]	0.15 ± 0.02	0.080 ± 0.006	0.045 ± 0.010	0.044 ± 0.003	2.9 ± 0.4	>100
4[b]	5.2 ± 1.0	1.6 ± 0.5	1.2 ± 0.2	0.73 ± 0.13	5.5 ± 0.7	>100
5[b]	10 ± 3	2.9 ± 1.0	3.7 ± 0.8	2.4 ± 0.2	31 ± 1	>100
7	7.7 ± 0.9	0.75 ± 0.10	0.39 ± 0.14	0.20 ± 0.09	58 ± 8	39 ± 12

[a] Mean ± SD from at least three experiments conducted in triplicate. [b] Reference 9.

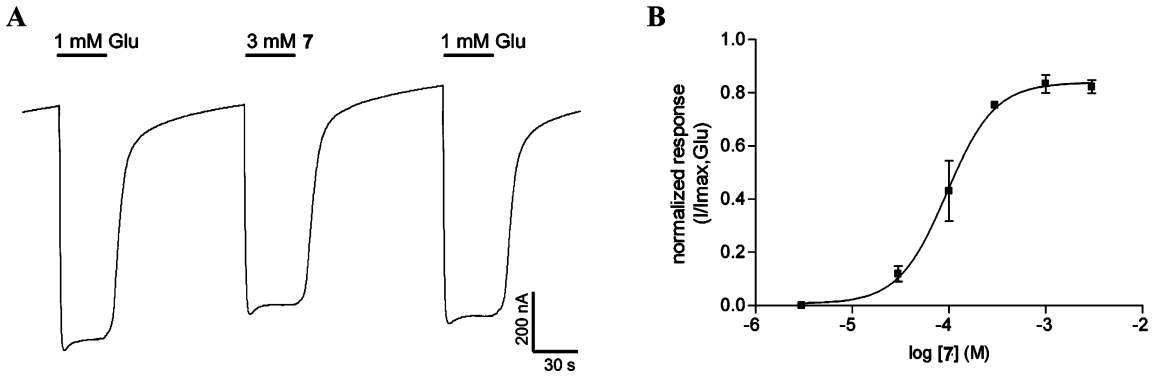

Figure 2. (A) Representative maximum currents evoked by **7** and Glu obtained from a two-electrode voltage clamp recording on a *Xenopus laevis* oocyte expressing GluR2$_o$ L483Y. (B) Concentration−response curves of **7** at GluR2$_o$ L483Y. The curves are normalized to the I_{max} of Glu.

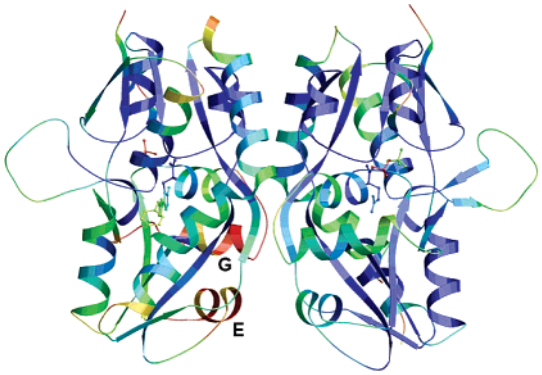

Figure 3. Cartoon representation of the overall structure of the GluR2-S1S2J dimer. Right protomer: molA containing Glu; left protomer: molB containing the (*S*)-form of the partial agonist **7**. The structure has been colored by *B*-values (blue are low and red are high values, ranging from 5 to 54 Å^2). The two ligands as well as three sulfate ions are shown in ball-and-stick representation.

structure of **2** bound to the GluR2-S1S2J construct[11] (Figure 4) (see Supporting Information for details). The isoxazole ring of **2** interacts with the protein through water molecule W7.[11] However, W7 is not present in the complex of (*S*)-**7** since a change in orientation of residue Thr686 eliminates the possibility for hydrogen-bond formation (Figure 4, 5A). Consequently, water molecule W2 in the present structure is observed relatively closer to the position of the previously observed W7. Thus, W2 has gained favorable contacts to the isoxazole ring (Figure 5A).

The 2-substituted tetrazole ring of (*S*)-**7** is not involved in hydrogen bonding but rather locked between the residues Glu402, Tyr405, Tyr450, Pro478, and Tyr732 of domain 1 (D1) and Thr686, Leu704, Glu705, and Met708 of domain 2 (D2) similar to what was observed in the case of **2** in GluR2-S1S2J.[11] The benzyl moiety of the ligand is partly located in the same cavity, but also reaches into a new area of the LBD in which substituents of agonists have not previously been observed (Figure 4B). Here, the aromatic ring of the benzyl moiety has

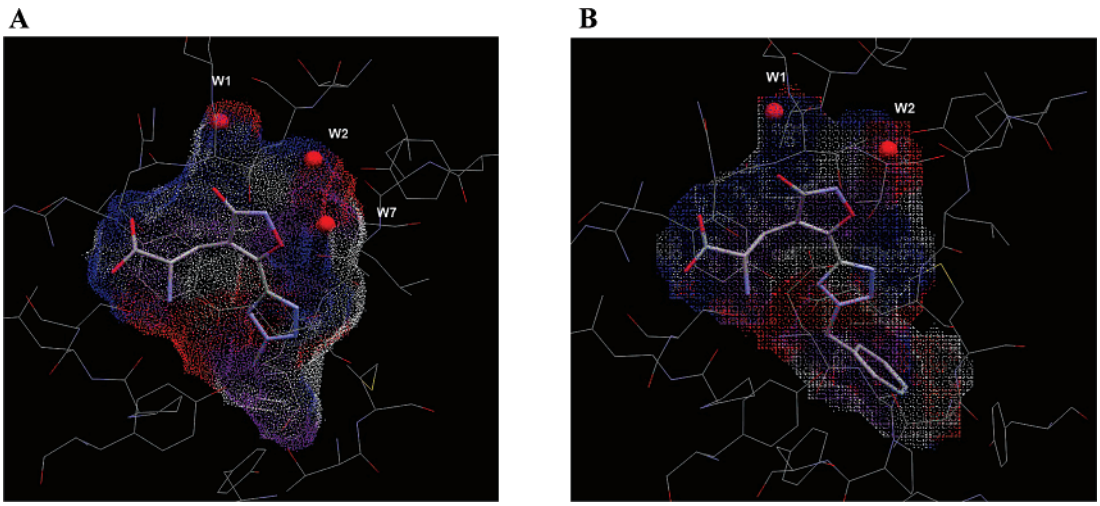

Figure 4. The LBD cavities of GluR2-S1S2J in complex with (A) **2** and (B) (*S*)-**7** as generated using CavBase.[30] Protein donor sites are displayed in blue, acceptor sites in red, donor−acceptor sites in magenta, and aliphatic/aromatic/π sites in white. The ligands are shown in stick representation and colored according to atom-type.

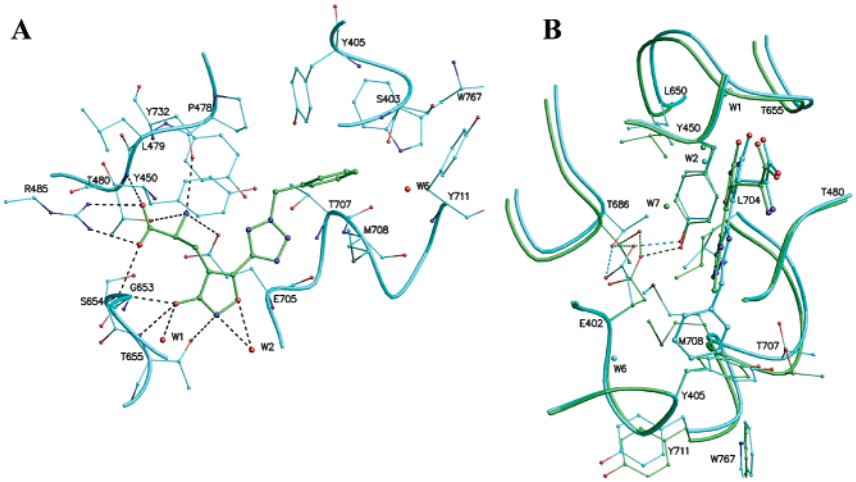

Figure 5. Binding mode of the (*S*)-form of the agonist **7** to GluR2-S1S2J. (A) Close-up view of the ligand-binding site, including potential hydrogen bonds within 3.5 Å (stippled lines). The ligand is shown in green and selected amino acid residues in cyan. Water molecules are displayed as red spheres. (B) Superposition of the GluR2-S1S2J structures in complex with (*S*)-**7** (cyan) and **2** (green), respectively. Selected side chains in vicinity of the ligands are shown. Water molecules are displayed as spheres and colored according to the structures. The hydrogen-bonding network between residues Glu402, Tyr450, and Thr686 is also indicated. Glu402 and Thr686 form the so-called interdomain lock between D1 and D2.

hydrophobic interactions with the residues Thr707 (D2), Tyr711 (D2) and Trp767 (D1) (Figure 5A). Compared with the structure of GluR2-S1S2J in complex with **2**, the new cavity is formed by the movement of Met708, which adopts a different conformation to accommodate the benzyl moiety (Figure 5B).

The side chains of residues Glu402 and Thr686 forming the so-called interdomain lock are also observed in different orientations in the two structures (Figure 5B). Thus, the carbon chain of Glu402 adopts a different conformation, whereas Thr686 flips 60° in the present structure. In the previous structure with **2**,[11] the interdomain lock can be described with one hydrogen bond between D1 and D2 from Glu402 OE2 to Thr686 OH (2.8 Å) and additional hydrogen bonds from Thr686 OH through water molecule W7 (2.8 Å) to Tyr702 OH (2.7 Å). In the present structure with (*S*)-**7**, a bidentate hydrogen bond is observed from Thr686 OH to the distal carboxylate of Glu402 (both 2.7 Å) (Figure 5B).

The domains of the LBD close upon agonist binding, sequestering the agonist in the cleft. Relative to the apo structure of GluR2-S1S2J (pdb-code 1FTO, molA), Glu induces 20.9° of domain closure in molA and (*S*)-**7** induces a domain closure of 21.5° in molB. When (*S*)-**7** binds to GluR2-S1S2J, it introduces some flexibility into the protomer (Figure 3); the average B value is 21 Å^2 compared with 16 Å^2 for the Glu-containing protomer. More flexibility is introduced in D2 (average B value of 25 Å^2) than in D1 (17 Å^2), primarily via helices E and G, which display high mobility (Figure 3).

As (*S*)-**7** crystallizes as a mixed dimer with Glu (even though Glu was not added during refolding and purification of GluR2-S1S2J and therefore must have been bound during protein expression), it indicates that this dimer is energetically most favorable at least under the present crystallization conditions. An additional data set was collected at EMBL, DESY, Hamburg, showing the same mixed dimer.

Molecular Modeling. A homology model of GluR1 in complex with (*S*)-**7** was built from molB by comparative modeling and side chain refinement in Prime 1.5.[21] Two methods were used to analyze the binding affinities of (*S*)-**7**, using default settings throughout. First, the ligand was redocked to molB and the GluR1 homology model using the recently described Glide 4.0 Extra Precision scoring function.[22] The RMSDs were within 0.25 Å of the experimental position in GluR2. A difference in Glidescore of −1.5, corresponding to 12-fold selectivity for GluR2 over GluR1 was noted, in good agreement with the experimental selectivity, and attributable primarily to a special electrostatic reward term present for GluR2 but not GluR1. The strongly negative score of −13.2 for (*S*)-**7** compared with the binding affinity at GluR2 is consistent with an energy cost associated with protein conformational rearrangement being required to bind this ligand. Second, the binding energies of the docked complexes with respect to the separated solvated ligand and protein were calculated by the Molecular Mechanics, Generalized Born/Solvent Accessibility method (MM-GBSA)[23] including the Surface Generalized Born (SGB) formalism[24] in Prime 1.5.[21] Briefly, this method estimates total binding free energy as the sum of the interaction energy according to OPLS2005 and the changes in solvation free energies and surface area contributions between the complex and separated protein and ligand, neglecting entropic corrections.[25] A $\Delta\Delta G$ of −2.2 kcal/mol was found in favor of binding to GluR2, primarily due to extra electrostatic stability of the GluR2:(*S*)-**7** complex vs the solvated *apo* protein compared with GluR1. Taken together, these results are consistent with fairly subtle electrostatic or solvent-driven effects contributing to selectivity, such as partial exposure of the benzyl group to a more strongly anionic environment in GluR1 (e.g., Asp399 and Glu683) in a fashion not previously seen for AMPA agonist complexes (Figure 6). Whereas previously observed selectivity preferences among GluR1−5 have generally been attributed to specific local polar[26] or steric[27] interactions, the influence of cumulative medium- to long-range effects including electrostatics is not without precedent in the glutamate field. For example, Poisson-Boltzmann electrostatics have been successfully used to describe the selectivities of a series of agonists at mGluR1, -2, and -4.[28]

Discussion

We have recently reported the synthesis and characterization of analogues of the potent AMPA receptor agonist **2** in which the methyl group at the tetrazole heterocycle was substituted with larger alkyl groups.[9] In this series of compounds the binding affinity decreased with increasing steric bulk of the alkyl group, but AMPA receptor agonism was observed for all analogues (Table 1). On the basis of molecular docking studies, we suspected that the volume of a benzyl substituent might exceed the limit for retaining agonist activity in this series.

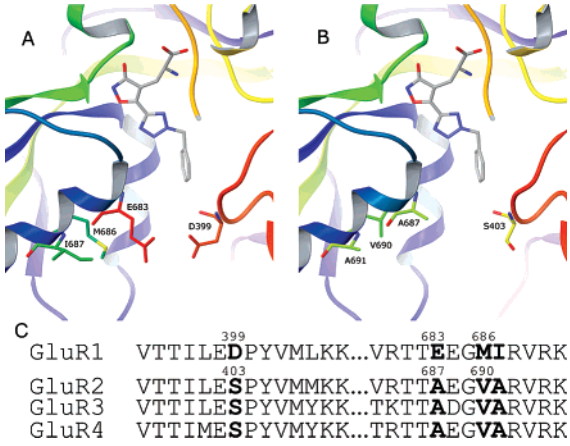

Figure 6. (A) Homology model of GluR1 highlighting nonconserved residues in the vicinity of bound (*S*)-**7**. (B) (*S*)-**7** docked to the experimental GluR2 structure. (C) Alignment of two regions of rat AMPA receptors GluR1−GluR4. The four residues located near the benzyl ring of (*S*)-**7** are highlighted. They are conserved in GluR2−4 but not in GluR1.

Instead, compound **7** turned out to also be an agonist. Moreover, compared with both the propyl- and isopropyl-substituted tetrazolyl AMPA analogues, **7** is more potent at GluR2−4, but has a similar low binding affinity at GluR1. At GluR4, compound **7** is only 5-fold less potent than AMPA. Consequently, compound **7** is the first AMPA receptor agonist to show the ability to significantly discriminate between GluR1 and GluR2, with an order of magnitude difference in affinity. Also with respect to GluR5, the selectivity for AMPA receptors is improved compared with the previous series.

Prompted by this interesting pharmacological profile of **7**, we obtained a crystal structure of the compound bound to GluR2 to explore the structural basis for the observed selectivity. We have previously reported the structure of **2** in GluR2-S1S2J,[11] where high complementarity between the ligand and the ligand-binding site of GluR2 is observed (Figure 4A). It is useful to compare this structure with the new structure containing (*S*)-**7**. The tetrazole rings of **2** and (*S*)-**7** are locked into the LBD in nearly the same manner, but there are notable differences between the two structures, imposed by the increased steric bulk of the benzyl group. Glu402 and Thr686, which form the so-called interdomain lock are observed in different orientations, and water molecule W7 is absent in the new structure. However, the most important difference is the movement of Met708, since this reorientation creates the entrance to a new cavity in the GluR2 binding domain that is unexplored by previous agonists. Thus, the size of the entire binding cavity increases when the ligand changes from **2** to **7** from 399 Å^3 to 492 Å^3 as calculated by the program Relibase+ with CavBase[29,30] (Figure 4).

All of the amino acids in contact with the benzyl moiety are conserved among the AMPA receptor subtypes including Thr686, Glu402, and Met708, which display altered conformations in the present crystal structure, and therefore none of these can account for the observed selectivity. However, in the present complex with **7**, Met708 approaches Val690 and Ala691, both of which are conserved in GluR2−4, but correspond to Met686 and Ile687, respectively, in GluR1 (Figure 6). In proximity to the benzyl group and neighboring Glu402 and Thr686 are the residues Ser403 and Ala687 that are also conserved in GluR2−4, but in GluR1 correspond to Asp399 and Glu683, respectively (Figure 6). The observed selectivity could therefore arise from these residues, for example if the hydrophobic benzyl group of **7** is partially exposed to this more anionic region in GluR1 by the analogous movement of Met686 (GluR1).

When the ligand binds to the LBD, domain closure presumably leads to opening of the ion channel. Ile633 is adjacent to the Gly-Thr (GT) linker and proximal to the transmembrane region that constitutes the ion channel, and the separation between these residues in the dimer depends on domain closure and seems to be coupled to the degree of channel activation.[31] Previously, linear relationships between agonist efficacy of the ligand, domain closure, and linker separation have been described.[31,32] The present dimer interface is as observed in other structures of GluR2 LBD complexes,[11,19] and the distance between the Cα atoms of Ile633 in each protomer is 35.6 Å (between Pro632 38.4 Å). This distance is intermediate between that observed in the Glu and **2** bound GluR2-S1S1J dimer structures, thus corresponding to a virtual heterodimer containing these two compounds. It is therefore likely that a homodimer containing only (*S*)-**7** would have a GT distance corresponding to that observed in the dimer containing **2**. Thus, both the separation of the GT linkers and the domain closure would predict a full agonist, but although **7** is highly efficacious it only induces 84% conductance relative to the conductance induced by the full agonist Glu (Figure 2). Obviously, other factors must account for the slightly reduced agonist efficacy of compound **7** compared to **2**. It is tempting to speculate that the decreased efficacy can be correlated with the observed increased mobility of helices E and G (Figure 3) close to the GT linker representing the connection to the ion-channel or that **7**, in addition to the closure revealed by the crystal structure, also may stabilize less closed domain conformations.

In conclusion, we have reported the synthesis and pharmacological characterization of the first AMPA receptor agonist that significantly differentiates between GluR1 and GluR2−4. This is a novel pharmacological profile among selective AMPA receptor agonists. The crystal structure of the GluR2-S1S2J construct containing (*S*)-**7** reveals that selectivity might be linked to the movement of several residues exposing a new pocket in the GluR2 LBD. Although the residues with altered conformations are conserved, adjacent residues are nonconserved in GluR1 compared with GluR2−4. Thus, compound **7** provides a new pharmacological tool with which to investigate the role of AMPA receptor subtypes and has induced a novel pocket in the LBD where sequence differences between GluR1−4 may be exploited further, with a view to designing ligands with increased AMPA subtype selectivity.

Experimental Section

***tert*-Butyl (*RS*)-2-(*N*-*tert*-butoxycarbonylamino)-3-[3-isopropoxy-5-(1-benzyl-1*H*-5-tetrazolyl)-4-isoxazolyl]propionate (9) and *tert*-Butyl (*RS*)-2-(*N*-*tert*-butoxycarbonylamino)-3-[3-isopropoxy-5-(2-benzyl-2*H*-5-tetrazolyl)-4-isoxazolyl]propionate (10).** *tert*-Butyl (*RS*)-2-(*N*,*N*-di-*tert*-butoxycarbonylamino)-3-[3-isopropoxy-5-(1*H*-5-tetrazolyl)-4-isoxazolyl]propionate[9] (250 mg, 0.47 mmol) and *O*-benzyl *S*-propargyl xanthate[12] (207 mg, 0.93 mmol) were dissolved in toluene (5 mL) and refluxed for 5 h. The solvent was removed *in vacuo*, and column chromatography (CC) (4:1 pentane/ EtOAc) afforded a 1:2 mixture (based on ^{1}H NMR) of the 1-tetrazolyl (**9**) and 2-tetrazolyl (**10**) regioisomers, respectively (227 mg, 0.43 mmol, 91%), as an oil.

***tert*-Butyl (*RS*)-2-(*N*,*N*-di-*tert*-butoxycarbonylamino)-3-[3-isopropoxy-5-(1-benzyl-1*H*-5-tetrazolyl)-4-isoxazolyl]propionate (11) and *tert*-Butyl (*RS*)-2-(*N*,*N*-di-*tert*-butoxycarbonylamino)-3-[3-isopropoxy-5-(2-benzyl-2*H*-5-tetrazolyl)-4-isoxazolyl]propionate (12).** *tert*-Butyl (*RS*)-2-(*N*,*N*-di-*tert*-butoxycarbonylamino)-3-[3-isopropoxy-5-(1*H*-5-tetrazolyl)-4-isoxazolyl]propionate[9] (400 mg, 0.74 mmol) was dissolved in dry THF (20 mL), and

triphenylphosphine (298 mg, 1.12 mmol), diisopropyl azodicarboxylate (216 μL, 1.12 mmol), and benzyl alcohol (115 μL, 1.12 mmol) were added. The solution was stirred at room temperature, under nitrogen for 30 min. The solvent was removed *in vacuo*, and CC (heptane to EtOAc) afforded a 1:2 mixture of **11** and **12** (420 mg, 88%) as an oil.

(*RS*)-2-Amino-3-[3-hydroxy-5-(1-benzyl-1*H*-5-tetrazolyl)-4-isoxazolyl]propionic Acid (6) and (*RS*)-2-Amino-3-[3-hydroxy-5-(2-benzyl-2*H*-5-tetrazolyl)-4-isoxazolyl]propionic Acid (7). Method A: A solution of **9** and **10** (227 mg, 0.43 mmol) in aqueous HBr (48 mL, 1 mL) was refluxed in a preheated 140 °C oil bath for 20 min. The solution was cooled, the solvent was removed *in vacuo*, and the residue was evaporated with water (3 × 5 mL). The residue was purified by reverse phase HPLC (see Supporting Information) and recrystallized (water/2-propanol) to give **7** (32 mg, 23%) as white crystals. The 1-regioisomer **6** was not present in detectable amounts.

Method B: A solution of precooled boron tribromide (1 M in CH_2Cl_2, 2.9 mL, 2.9 mmol) was carefully added to a mixture of **11** and **12** (366 mg, 0.58 mmol) in CH_2Cl_2 (1 mL) at −78 °C. The solution was allowed to warm to room temperature over 5 h. The reaction was quenched with saturated NH_4Cl (1 mL), the aqueous phase was washed with CH_2Cl_2, and the solvent removed *in vacuo* to give a crude mixture of **6** and **7**. The two isomers were separated and purified by reversed phase HPLC (see Supporting Information) and recrystallized (water/2-propanol) to give **6** (36 mg, 19%) and **7** (54 mg, 28%).

Acknowledgment. Veronica Nuvoloni is gratefully thanked for assistance with the final purification of **7**. Lise Baadsgaard Sørensen is gratefully thanked for crystallization of the complex and Desiree Sprogøe for mounting the crystals for data collection. This work was supported by grants from the Lundbeck Foundation and the Novo Nordisk Foundation. We also acknowledge financial support from the Danish Medical Research Foundation, DANSYNC (Danish Center for Synchrotron-Based Research), and The European Community - Access to Research Infrastructure Action of the Improving Human Potential Program to the EMBL Hamburg Outstation.

Supporting Information Available: NMR spectra for compounds **6**, **7**, **9**−**12**, homology model of (*S*)-**7**:GluR1, and experimental procedures for HPLC, *in vitro* pharmacology, and X-ray crystallography. This material is available free of charge via the Internet at http://pubs.acs.org.

References

(1) Bräuner-Osborne, H.; Egebjerg, J.; Nielsen, E. Ø.; Madsen, U.; Krogsgaard-Larsen, P. Ligands for glutamate receptors: Design and therapeutic prospects. *J. Med. Chem.* **2000**, *43*, 2609−2645.
(2) Dingledine, R.; Borges, K.; Bowie, D.; Traynelis, S. F. The glutamate receptor ion channels. *Pharmacol. Rev.* **1999**, *51*, 7−61.
(3) Riedel, G.; Platt, B.; Micheau, J. Glutamate receptor function in learning and memory. *Behav. Brain Res.* **2003**, *140*, 1−47.
(4) Javitt, D. C. Glutamate as a therapeutic target in psychiatric disorders. *Mol. Psychiatry* **2004**, *9*, 984−997.
(5) Erreger, K.; Chen, P. E.; Wyllie, D. J.; Traynelis, S. F. Glutamate receptor gating. *Crit. Rev. Neurobiol.* **2004**, *16*, 187−224.
(6) Magri, C.; Gardella, R.; Barlati, S. D.; Podavini, D.; Iatropoulos, P.; Bonomi, S.; Valsecchi, P.; Sacchetti, E.; Barlati, S. Glutamate AMPA receptor subunit 1 gene (GRIA1) and DSM-IV-TR schizophrenia: A pilot case-control association study in an Italian sample. *Am. J. Med. Genet. B Neuropsychiatr. Genet.* **2006**, *141*, 287−293.
(7) Bang-Andersen, B.; Lenz, S. M.; Skjærbæk, N.; Søby, K. K.; Hansen, H. O.; Ebert, B.; Bøgesø, K. P.; Krogsgaard-Larsen, P. Heteroaryl analogues of AMPA. Synthesis and quantitative structure-activity relationships. *J. Med. Chem.* **1997**, *40*, 2831−2842.
(8) Vogensen, S. B.; Jensen, H. S.; Stensbøl, T. B.; Frydenvang, K.; Bang-Andersen, B.; Johansen, T. N.; Egebjerg, J.; Krogsgaard-Larsen, P. Resolution, configurational assignment, and enantiopharmacology of 2-amino-3-[3-hydroxy-5-(2-methyl-2*H*-tetrazol-5-yl]isoxazol-4-yl]-propionic acid, a potent GluR3- and GluR4-preferring AMPA receptor agonist. *Chirality* **2000**, *12*, 705−713.
(9) Vogensen, S. B.; Clausen, R. P.; Greenwood, J. R.; Johansen, T. N.; Pickering, D. S.; Nielsen, B.; Ebert, B.; Krogsgaard-Larsen P. Convergent synthesis and pharmacology of substituted tetrazolyl-2-amino-3-(3-hydroxy-5-methyl-4-isoxazolyl)propionic acid analogues. *J. Med. Chem.* **2005**, *48*, 3438−3442.
(10) Bjerrum, E. J.; Kristensen, A. S.; Pickering, D. S.; Greenwood, J. R.; Nielsen, B.; Liljefors, T.; Schousboe, A.; Bräuner-Osborne, H.; Madsen, U. Design, synthesis, and pharmacology of a highly subtype-selective GluR1/2 agonist, (*RS*)-2-amino-3-(4-chloro-3-hydroxy-5-isoxazolyl)propionic acid (Cl-HIBO). *J. Med. Chem.* **2003**, *46*, 2246−2249.
(11) Hogner, A.; Kastrup, J. S.; Jin, R.; Liljefors, T.; Mayer, M. L.; Egebjerg, J.; Larsen, I. K.; Gouaux, E. Structural basis for AMPA receptor activation and ligand selectivity: Crystal structures of five agonist complexes with the GluR2 ligand-binding core. *J. Mol. Biol.* **2002**, *322*, 93−109.
(12) Fauré-Tromeur, M.; Zard S. Z. A practical synthesis of benzyl esters and related derivatives. *Tetrahedron Lett.* **1998**, *39*, 7301−7304.
(13) Honore, T.; Nielsen, M. Complex structure of quisqualate-sensitive glutamate receptors in rat cortex. *Neurosci. Lett.* **1985**, *54*, 27−32.
(14) Braitman, D. J.; Coyle, J. T. Inhibition of [^{3}H]kainic acid receptor binding by divalent cations correlates with ion affinity for the calcium channel. *Neuropharmacology* **1987**, *26*, 1247−1251.
(15) Sills, M. A.; Fagg, D.; Pozza, M.; Angst, C.; Brundish, D. E.; Hurt, S. D.; Wilusz, E. J.; Williams, M. [^{3}H]CGP 39653: a new *N*-methyl-D-aspartate antagonist radioligand with low nanomolar affinity in rat brain. *Eur. J. Pharmacol.* **1991**, *192*, 19−24.
(16) Ransom, R. W.; Stec N. L. Cooperative modulation of [^{3}H]MK801 binding to the *N*-methyl-D-aspartate receptor ion channel complex by L-glutamate, glycine and polyamines. *J. Neurochem.* **1988**, *51*, 830−836.
(17) Madsen, U.; Frølund, B.; Lund, T. M.; Ebert, B.; Krogsgaard-Larsen, P. Design, synthesis and pharmacology of model compounds for indirect elucidation of the topography of AMPA receptor sites. *Eur. J. Med. Chem.* **1993**, *28*, 791−800.
(18) Harrison, N. L.; Simmonds M. A. Quantitative studies on some antagonists of *N*-methyl-D-aspartate in slices of rat cerebral cortex. *Br. J. Pharmacol.* **1985**, *84*, 381−391.
(19) Armstrong, N.; Gouaux, E. Mechanisms for activation and antagonism of an AMPA-sensitive glutamate receptor: Crystal structures of the GluR2 ligand binding core. *Neuron* **2000**, *28*, 165−181.
(20) Kasper, C.; Lunn, M. L.; Liljefors, T.; Gouaux, E.; Egebjerg, J.; Kastrup, J. S. GluR2 ligand-binding core complexes: importance of the isoxazolol moiety and 5-substituent for the binding mode of AMPA-type agonists. *FEBS Lett.* **2002**, *531*, 173−178.
(21) Prime 1.5, Glide 4.0., Schrödinger Inc., 101 SW Main Street, Portland OR, 2006.
(22) Friesner, R. A.; Murphy, R. B.; Repasky, M. P.; Frye, L. L.; Greenwood, J. R.; Halgren, T. A.; Sanschagrin, P. C.; Mainz, D. T. Extra precision glide: Docking and scoring incorporating a model of hydrophobic enclosure for protein−ligand complexes. *J. Med. Chem.* **2006**, *49*, 6177−6196.
(23) Zou, X. Q.; Sun, Y. X.; Kuntz, I. D. Inclusion of solvation in ligand binding free energy calculations using the generalized-born model. *J. Am. Chem. Soc.* **1999**, *121*, 8033−8043.
(24) Yu, Z. Y.; Jacobson, M. P.; and Friesner, R. A. What role do surfaces play in GB models? A new-generation of surface-generalized Born model based on a novel Gaussian surface for biomolecules. *J. Comput. Chem.* **2006**, *27*, 72−89.
(25) Huang, N.; Kalyanaraman, C.; Bernacki, K.; Jacobson, M. P. Molecular mechanics methods for predicting protein-ligand binding. *Phys. Chem. Chem. Phys.* **2006**, *8*, 5166−5177.
(26) Greenwood, J. R.; Mewett, K. N.; Allan, R. D.; Martin, B. O.; Pickering, D. S. 3-hydroxypyridazine 1-oxides as carboxylate bioisosteres: A new series of subtype-selective AMPA receptor agonists. *Neuropharmacology* **2006**, *51*, 52−59.
(27) Brehm, L.; Greenwood, J. R.; Hansen, K. B.; Nielsen, B.; Egebjerg, J.; Stensbøl, T. B.; Bräuner-Osborne, H.; Sløk, F.; Kronborg, T. T. A.; Krogsgaard-Larsen, P. (*S*)-2-amino-3-(3-hydroxy-7,8-dihydro-6H-cyclohepta[d]isoxazol-4-yl)propionic acid, a potent and selective agonist at the GluR5 subtype of ionotropic glutamate receptors. Synthesis, modeling, and molecular pharmacology. *J. Med. Chem.* **2003**, *46*, 1350−1358.
(28) Macchiarulo, A.; Constantino, G.; Sbaglia, R.; Aiello, S.; Meniconi, M.; Pellicciari, R. The role of electrostatic interaction in the molecular recognition of selective agonists to metabotropic glutamate receptors. *Proteins Struct. Funct. Genet.* **2003**, *50*, 609−619.
(29) Hendlich, M.; Bergner, A.; Gunther, J.; Klebe, G. Relibase: Design and development of a database for comprehensive analysis of protein-ligand interactions. *J. Mol. Biol.* **2003**, *326*, 607−620.
(30) Schmitt, S.; Kuhn, D.; Klebe, G. CavBase: A new method to detect related function among proteins independent of sequence and fold homology. *J. Mol. Biol.* **2002**, *323*, 387−406.

(31) Frandsen, A.; Pickering, D. S.; Vestergaard, B.; Kasper, C.; Nielsen, B. B.; Greenwood, J. R.; Campiani, G.; Fattorusso, C.; Gajhede, M.; Schousboe, A.; Kastrup, J. S. Tyr702 is an important determinant of agonist binding and domain closure of the ligand-binding core of GluR2. *Mol. Pharmacol.* **2005**, *67*, 703−713.

(32) Jin, R. S.; Banke, T. G.; Mayer, M. L.; Traynelis, S. F.; Gouaux, E. Structural basis for partial agonist action at ionotropic glutamate receptors. *Nat. Neurosci.* **2003**, *6*, 803−810.

JM061439Q